Am J Physiol Heart Circ Physiol 289: H1291–H1300, 2005.
First published April 29, 2005; doi:10.1152/ajpheart.00111.2005.

A novel model of cryoinjury-induced myocardial infarction in the mouse: a comparison with coronary artery ligation

Ewout J. van den Bos,[1] Barend M. E. Mees,[2,3] Monique C. de Waard,[1] Rini de Crom,[2,3] and Dirk J. Duncker[1]

[1]*Experimental Cardiology, Thoraxcenter,* [2]*Department of Cell Biology and Genetics, and* [3]*Department of Vascular Surgery, Cardiovascular Research School Coeur, Erasmus MC, University Medical Center, Rotterdam, The Netherlands*

Submitted 3 February 2005; accepted in final form 21 April 2005

Van den Bos, Ewout J., Barend M. E. Mees, Monique C. de Waard, Rini de Crom, and Dirk J. Duncker. A novel model of cryoinjury-induced myocardial infarction in the mouse: a comparison with coronary artery ligation. *Am J Physiol Heart Circ Physiol* 289: H1291–H1300, 2005. First published April 29, 2005; doi:10.1152/ajpheart.00111.2005.—Mouse myocardial infarction (MI) models are frequently used research tools. The most commonly applied model is coronary artery ligation. However, coronary ligation often gives rise to apical aneurysmatic infarcts of variable size. Other infarct models include cryoinfarction, which produces reproducible infarcts of the anterior wall. Thus far, this model has not been extensively described in mice. Therefore, we developed a murine cryoinfarction model and compared it with coronary ligation. Studies were performed under isoflurane anesthesia with a follow-up of 4 and 8 wk. Cryoinfarction was induced using a 2- or 3-mm cryoprobe. Two-dimensional guided M-mode echocardiography was used to assess fractional shortening and left ventricular (LV) dimensions at baseline and end point. At end point, hemodynamics were assessed using a 1.4-Fr Millar catheter. Pressure-diameter relations were constructed by combining echocardiography and hemodynamic data. Histological and morphometric analyses of infarct and remote areas were performed. At 4 wk, 3-mm cryoinfarction resulted in decreased LV fractional shortening as well as decreased global LV contractility and relaxation, which was comparable with coronary ligation. No adverse remodeling was observed at this time point, in contrast with the ligation model. However, progressive LV remodeling occured between 4 and 8 wk after cryoinfarction with a further decline in hemodynamic parameters and LV pump function. Histologically, cryoinfarction resulted in highly reproducible, transmural, cone-shaped infarcts with reperfusion at the macrovascular level. These results indicate that the cryoinfarction model represents the anterior myocardial infarct with modest adverse remodeling and may thus be representative for infarcts encountered in clinical practice.

heart function; cardiac remodeling; echocardiography

WITH THE ACCUMULATING AVAILABILITY of various models of genetically modified mice, there is a growing interest in murine models of myocardial infarction (MI) for the study of cardiac remodeling (18). The most widely studied model of murine MI is permanent ligation of the left anterior descending coronary artery (LAD) (12, 16). Although highly representative of ischemic cell death as occurs in humans, the ligation model is inherently associated with infarcts of variable size, requiring large group numbers of mice in studies that evaluate antiremodeling therapies. Even more importantly, LAD ligation in the mouse heart typically leads to apical infarcts with large aneurysm formation causing a particular ventricular geometry. Ligation-induced infarcts in the mouse heart appear therefore less representative for infarcts encountered in clinical practice, where acute LAD occlusion followed by aggressive reperfusion therapy often leads to moderately sized infarcts of the anterior free wall.

Several alternative models of MI have been proposed and studied over the years in various animal models, including infarction by freeze-thaw injury, or cryoinjury (2, 20). In the last years, cryoinjury has been mainly applied in studies on intracardiac cell transplantation (9, 14, 15, 21). However, to date, no study has been performed to elucidate the effects of cryoinjury on infarct size, heart function, and left ventricular (LV) remodeling in the mouse. In this study, we examined the effects of cryoinjury using echocardiography, hemodynamic measurements, pressure-diameter relations, and histology and compared these with results from coronary artery ligation.

METHODS

Animals. All animal experiments were performed in accordance with the National Institutes of Health *Guide for the Care and Use of Laboratory Animals* (NIH Pub. No. 86-23, Revised 1996) and with prior approval of the Animal Care Committee of the Erasmus MC. Mice (C57Bl6) were ~10 wk of age at the start of the experimental protocol. Experiments were performed using both male and female mice at random.

Echocardiography. Mice were weighed, anesthetized with isoflurane, and intubated using a 24-gauge intravenous catheter with a blunt end. Mice were artificially ventilated with a mixture of O_2 and N_2O [1:2 (vol/vol)] to which isoflurane [2.5–3.0% (vol/vol)] was added at a rate of 80 strokes/min using a rodent ventilator (SAR-830/P, CWE; Ardmore, PA) at an inspiratory pressure of 18 cmH_2O. The mouse was placed on a heating pad to maintain body temperature at 37°C. The chest was dehaired using Veet hair removal (Reckitt Benckiser; Parsippany, NJ). Echocardiograms were obtained with an Aloka SSD 4000 echo device (Aloka; Tokyo, Japan) using a 12-MHz probe. Images of the short and long axis were obtained in two-dimensional and M-mode settings with simultaneous echocardiographic gating as described previously (6, 19).

Cryoinfarction. A thoracotomy was performed through the fourth left intercostal space, the pericardium was opened, and the heart was exposed. Cryoinfarction was produced by applying a cryoprobe of 2 or 3 mm in diameter (Cry-AC-3 B-800, Brymill Cryogenic Systems; Basingstoke, UK) (Fig. 1) to the anterior LV free wall followed by freezing for 10 s. The exact position of the probe was carefully set using the left atrium and pulmonary artery as anatomic landmarks.

Address for reprint requests and other correspondence: D. J. Duncker, Experimental Cardiology, Thoraxcenter, Erasmus MC, Univ. Medical Center, Rm. Ee 2355, PO Box 1738, Rotterdam 3000 DR, The Netherlands (E-mail: d.duncker@erasmusmc.nl).

The costs of publication of this article were defrayed in part by the payment of page charges. The article must therefore be hereby marked "*advertisement*" in accordance with 18 U.S.C. Section 1734 solely to indicate this fact.

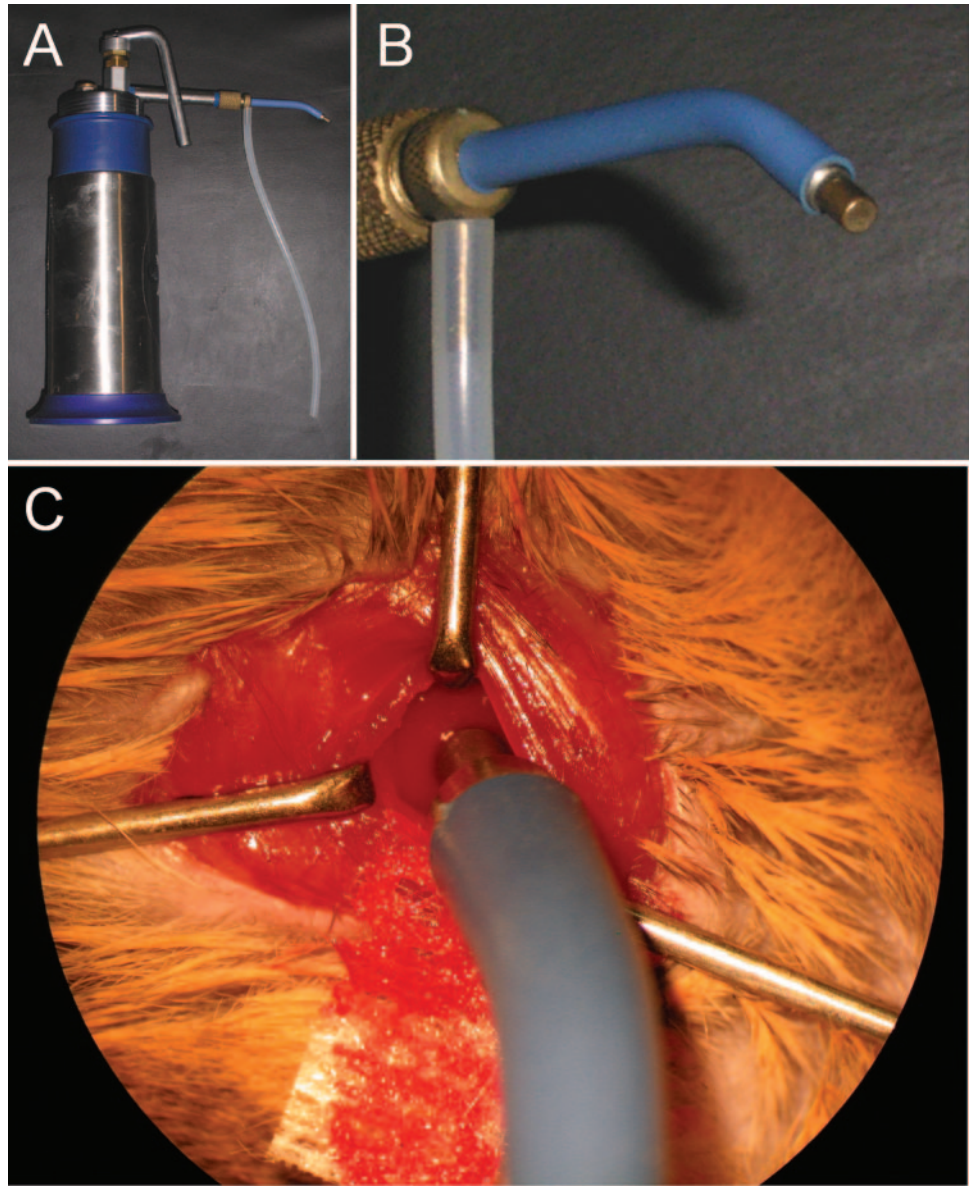

Fig. 1. *A*: cryoprobe used in this study. *B*: enlargement of the probe end of the 3-mm model. *C*: the thoracotomy as seen through the stereomicroscope; the probe can be seen in contact with the anterior wall moments before freezing.

Rinsing with saline at room temperature was performed to allow nontraumatic detachment of the probe from the LV wall after the freezing.

LAD ligation. Ligation of the LAD was performed as described previously (3, 12, 16). Briefly, a thoracotomy was performed through the fourth left intercostal space, and the proximal LAD (12, 16) was permanently ligated by passing a 7-0 silk suture mounted on a tapered needle (BV-1, Ethicon; Somerville, NJ) around the artery. Sham animals underwent a thoracotomy without infarct induction. Control animals did not undergo any surgery.

Hemodynamic measurements. Either 4 wk or 8 wk after infarction, echocardiography was repeated under anesthesia as described above. After echocardiography, mice were instrumented for hemodynamic measurements. For this purpose, a polyethylene catheter (PE-10) was inserted into the left carotid artery and advanced into the aortic arch to measure aortic blood pressure. A 1.4-Fr microtipped manometer (Millar Instruments; Houston, TX) (calibrated before each experiment with a mercury manometer) was inserted via the right carotid artery and advanced into the LV lumen to measure LV pressure and its first derivative (LV dP/dt). Subsequently, baseline recordings were obtained of aortic blood pressure, heart rate (HR), and LV pressure.

Data analysis. Echocardiography data were stored for off-line analysis. LV end-diastolic (EDD) and end-systolic diameters (ESD) were measured from the M-mode images using Sigmascan Pro 5.0 Image Analysis software (SPSS; Chigago, IL). Three consecutive beats were analyzed by a blinded observer. Twenty-one animals were randomly selected for analysis by a second blinded observer to calculate interobserver variability. LV absolute shortening (EDD − ESD) and fractional shortening [FS = (EDD − ESD)/EDD × 100%] were calculated. Hemodynamic data were recorded and digitized (sampling rate of 5,000 s^{-1} per channel) using an on-line four-channel data-acquisition program (ATCODAS, Dataq Instruments; Akron, OH) for postacquisition off-line analysis with a program written in MATLAB (Mathworks; Natick, MA). Ten consecutive beats were selected for the determination of HR, LV peak systolic (LVSP), LV end-diastolic pressures (LVEDP), diastolic aortic pressure (DAP), and the maximum rates of rise (LV dP/dt_{max}) and fall (LV dP/dt_{min}) of LV pressure as well as the rate of rise of LV pressure at a pressure of 30 mmHg (LV dP/dt_{P30}). In addition, the time constant of LV pressure decay (τ), an index of early LV relaxation, was computed as described previously (6, 23).

Pressure-diameter relations were constructed with a program written in MATLAB using the electrocardiographic signal for synchronization of the echocardiography M-mode dataset and the LV pressure signal. Data from four consecutive beats were averaged.

Infarct reperfusion, histology, and morphometric measurements. At the conclusion of each experiment, the heart and lungs were excised. The right ventricle and atria were removed. Wet weights of the LV and right ventricle and lungs as well as tibia length were determined. The area of cryoinfarction could be easily identified macroscopically. The LV was cut in two halves through the center of the infarct along the longitudinal axis. The half of the LV comprising the interventricular septum was fixed overnight in freshly prepared paraformaldehyde (4%) in PBS. Paraffin sections from the infarct center were stained with hematoxylin-eosin (HE) and Masson's trichrome (MT). Sections were photographed using an Olympus BH 20 microscope (Olympus; Tokyo, Japan) and analyzed using Clemex Vision PE analysis software (Clemex Technologies; Longueuil, Quebec, Canada). The infarct region was demarcated, and the area was measured. Endocardial and epicardial infarct circumference were demarcated, and the lengths were measured. Infarct thickness was measured at the shortest distance between the endocardium and epicardium. Cardiomyocyte size in the noninfarcted interventricular septum, i.e., remote myocardium, was determined by cross-sectional area measurements of cardiomyocytes in transverse orientation and at identical magnification (11).

The other half of the LV was embedded in optimal cutting temperature (OCT) compound (Tissue Tek, Sakura; Zoeterwoude, The Netherlands) and frozen in liquid nitrogen-cooled isopentane. Frozen sections were cut, air dried, and fixed in acetone. Slides were then incubated with anti-CD31 antibody (Pharmingen; San Diego, CA) for 1 h, followed by an incubation with goat anti-rat secondary antibody (Alex Fluor 568, Molecular Probes; Leiden, The Netherlands). Staining was analyzed using fluorescence microscopy (Axiovert S100, Zeiss; Oberkochen, Germany). Four to five images comprising the whole infarct area were taken at ×200. CD31-positive vessels were counted in each field, vessel areas were measured using Clemex Vision PE analysis software, and both were expressed as measures per unit area as described previously (24).

To study reperfusion of the infarct territory in a more acute post-MI phase, additional mice were killed 2 days after 3-mm cryoinfarction. Before death, either 50 μl thioflavin S (4% solution in saline, Sigma; St. Louis, MO; $n = 3$) or 50 μl Unisperse blue (50% suspension in saline, Ciba Specialty Chemicals; Maastricht, The Netherlands; $n = 3$) was injected into the right ventricular lumen. Thioflavin S-stained hearts were cut into four short-axis slices and photographed under ultraviolet light (365-nm wavelength). Unisperse blue-stained hearts were processed for HE staining following the same protocol as described above.

Additional mice were killed at 2 and 4 days for HE and MT staining only ($n = 3$ at each time point).

Statistics. Statistical analysis of all data was performed using one- or two-way ANOVA as appropriate, followed by Student-Newman-Keuls test or Tukey test. Analysis of echocardiographic data was performed using two-way ANOVA for repeated measures followed by Tukey test. Data are reported as means ± SE. Statistical significance was accepted when $P < 0.05$ (two-tailed). Statistical analysis was performed using SigmaStat version 2.03 software (SPSS; Chigago, IL). Kaplan-Meier curves were constructed using StatView version 5.0.1 software (SAS Institute; Cary, NC).

RESULTS

Survival. A total of 147 mice was used for the study. In the control, sham, and 2-mm cryoinfarction groups, all animals survived. Total periprocedural mortality (including the first 2 h postprocedure) in the 3-mm cryoinfarction groups and ligation groups was 8.7% and 12.5%, respectively. Total mortality during the follow-up period was significantly lower after cryoinfarction compared with coronary ligation (Fig. 2).

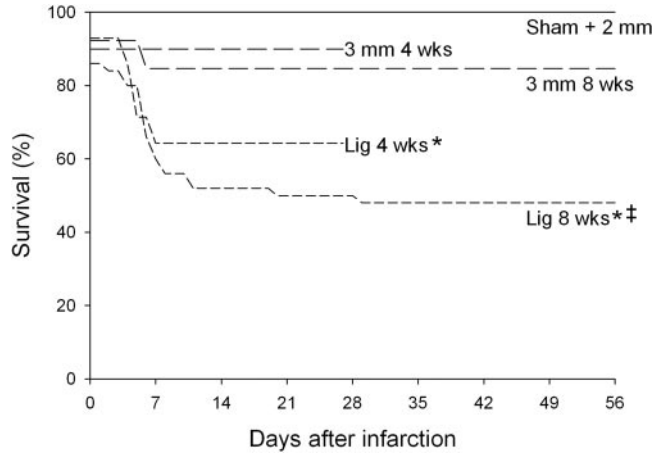

Fig. 2. Survival curves in the sham, 2-mm cryoinfarction (2 mm), 3-mm cryoinfarction (3 mm), and coronary ligation (Lig) groups after 4 and 8 wk. Kaplan-Meier analysis showed a significant decrease in survival after coronary ligation compared with cryoinfarction after 8 wk. *$P < 0.05$ vs. corresponding sham; ‡$P < 0.05$ vs. corresponding 3 mm.

Effect of surgery and gender. No significant differences between control ($n = 15$) and sham mice or between male and female mice were found in any of the hemodynamic or echocardiographic measurements.

Infarct reperfusion, infarct histology, and morphometry. Two days after cryoinfarction, large areas of no reflow were observed macroscopically within the infarct center and epicardial borders after thioflavin S staining (Fig. 3, *A* and *B*). However, the LAD and larger vessels were reperfused (Fig. 3, *C–E*). This was confirmed by Unisperse blue staining: only along the endocardial border were reperfused capillaries observed (Fig. 3, *F–H*).

Cryoinjury led to transmural MI in all animals (Fig. 4*A*). Four days after infarction, an extensive area of coagulation necrosis with hemorrhage was observed in the center of the cryoinfarcts. Furthermore, a dense inflammatory infiltrate could be observed (Fig. 4*C*). At higher magnification, vascular lacunae were visible with endothelial discontinuities (Fig. 4*D*). Four weeks after infarction, a transmural, paucicellular scar was formed, consisting of collagenous fibers with a short transition zone to healthy myocardium (Fig. 4, *E* and *F*). No surviving cardiomyocytes were observed within the infarct area or along the endocardial border. The LAD was patent in each cryoinfarcted animal at 4 and 8 wk as observed by open vessels filled with erythrocytes (Fig. 4*G*). In contrast, after coronary ligation, obliteration of the LAD and larger vessels was invariably observed (Fig. 4*H*).

Coronary ligation also resulted in transmural MI in all animals (Fig. 4*B*). However, along the endocardial wall and larger vessels, small islands of surviving cardiomyocytes were present. Epicardial and endocardial infarct border lengths were significantly larger in the ligation groups compared with the 2- and 3-mm cryoinfarction groups (Table 1). Furthermore, the ligation infarcts were significantly thinner at 4 wk compared with the cryoinfarction groups, and significant infarct thinning occurred between 4 and 8 wk in the ligation group. As a result, the ligation infarct areas were larger than the 3-mm cryoin-

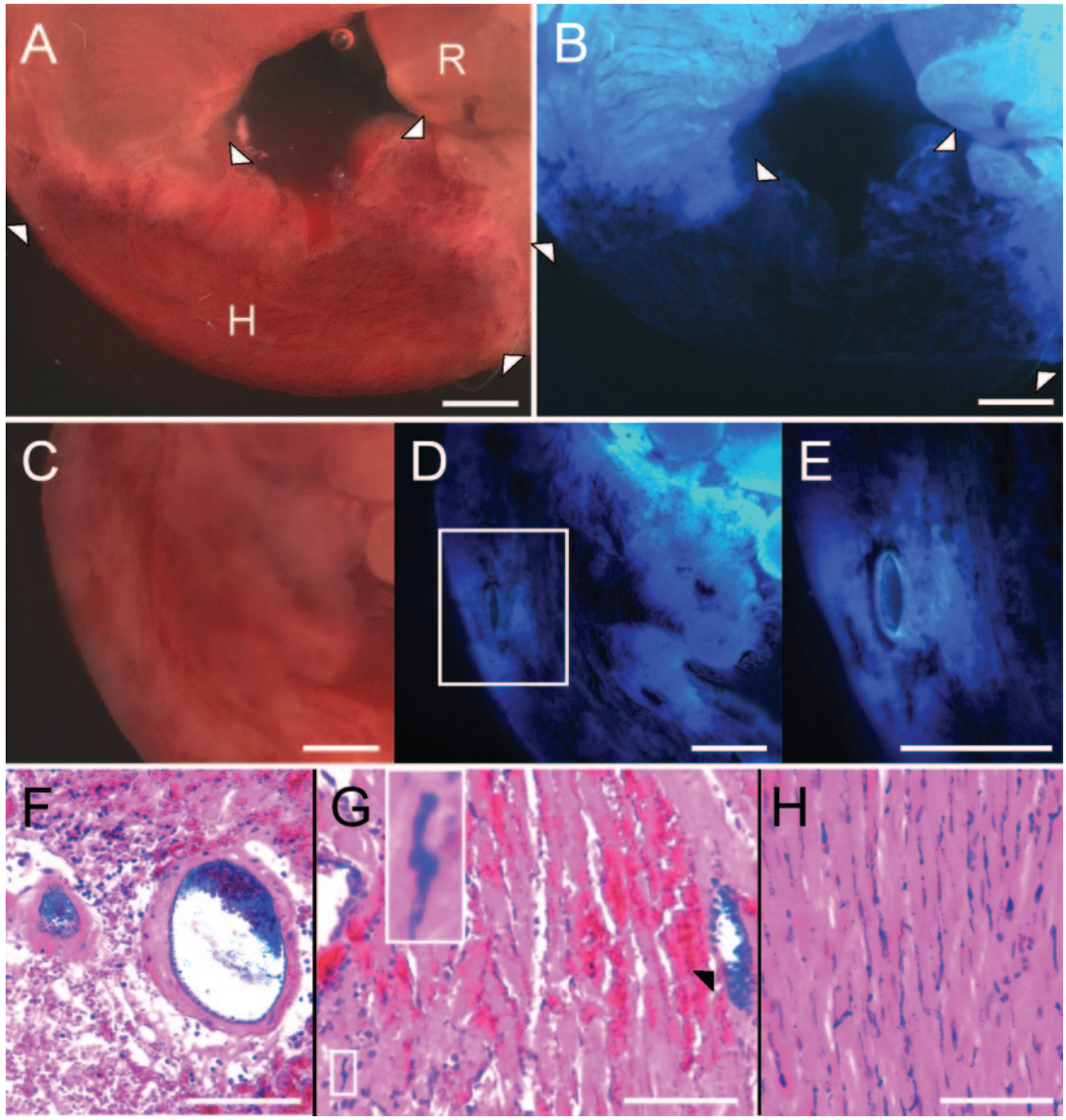

Fig. 3. *A*: 3-mm cryoinfarction after 2 days (delineated by white arrowheads). A large area of hemorrhage (H) occupies the infarct center; R indicates remote healthy myocardium. *B*: corresponding view under ultraviolet light. The infarct area is not stained by thioflavin S, indicating no reflow caused by microvascular damage. *C*: 3-mm cryoinfarction of a different heart. Less hemorrhage is visible. *D*: corresponding view under ultraviolet light. *E*: boxed region in *D* containing the left anterior descending coronary artery (LAD) shown at higher magnification. Both the LAD and a small region around it are reperfused. Unisperse blue was found in the LAD and larger vessels in all animals [arrowhead; *F* and *G*, hematoxylin-eosin (HE) stain]. Capillary reperfusion was selectively found along the endocardial borders (boxed region; *G*, HE stain). *H*: perfused capillaries in the remote noninfarcted myocardium (HE stain). Bars = 0.5 mm in *A–E* and 100 μm in *F–H*.

farcts at 4 and 8 wk, although these differences failed to reach statistical significance (Table 1).

Vessel density and area per vessel as assessed by CD31 immunohistochemistry were not significantly different between cryoinfarction and ligation groups. However, vessel area as a percentage of total tissue area was significantly lower in the ligation group compared with the cryoinfarction and sham groups (Fig. 5).

Systemic hemodynamics and LV pressure-derived indices of LV performance. Hemodynamic parameters are shown in Table 2. No significant differences between the groups were observed in HR or DAP. Four weeks after coronary ligation, a significant increase in LVEDP was observed compared with the sham and cryoinfarction groups. A small but significant difference in LVEDP between ligation and 3-mm cryoinfarction was still observed after 8 wk. In both the cryoinfarction and coronary ligation groups, a significant decrease in LVSP was observed after 4 wk compared with the sham group.

Four weeks after infarction, LV dP/dt_{max} was significantly reduced in the 3-mm cryoinfarction and ligation groups compared with the sham group, which corresponded with the changes in the afterload-independent parameter LV dP/dt_{P30}. At 8 wk, LV dP/dt_{max} and LV dP/dt_{P30} were identical in the 3-mm cryoinfarction and ligation groups (Fig. 6).

LV dP/dt_{min} was significantly reduced after 4 wk in the 2- and 3-mm cryoinfarction and ligation groups (Fig. 6), which

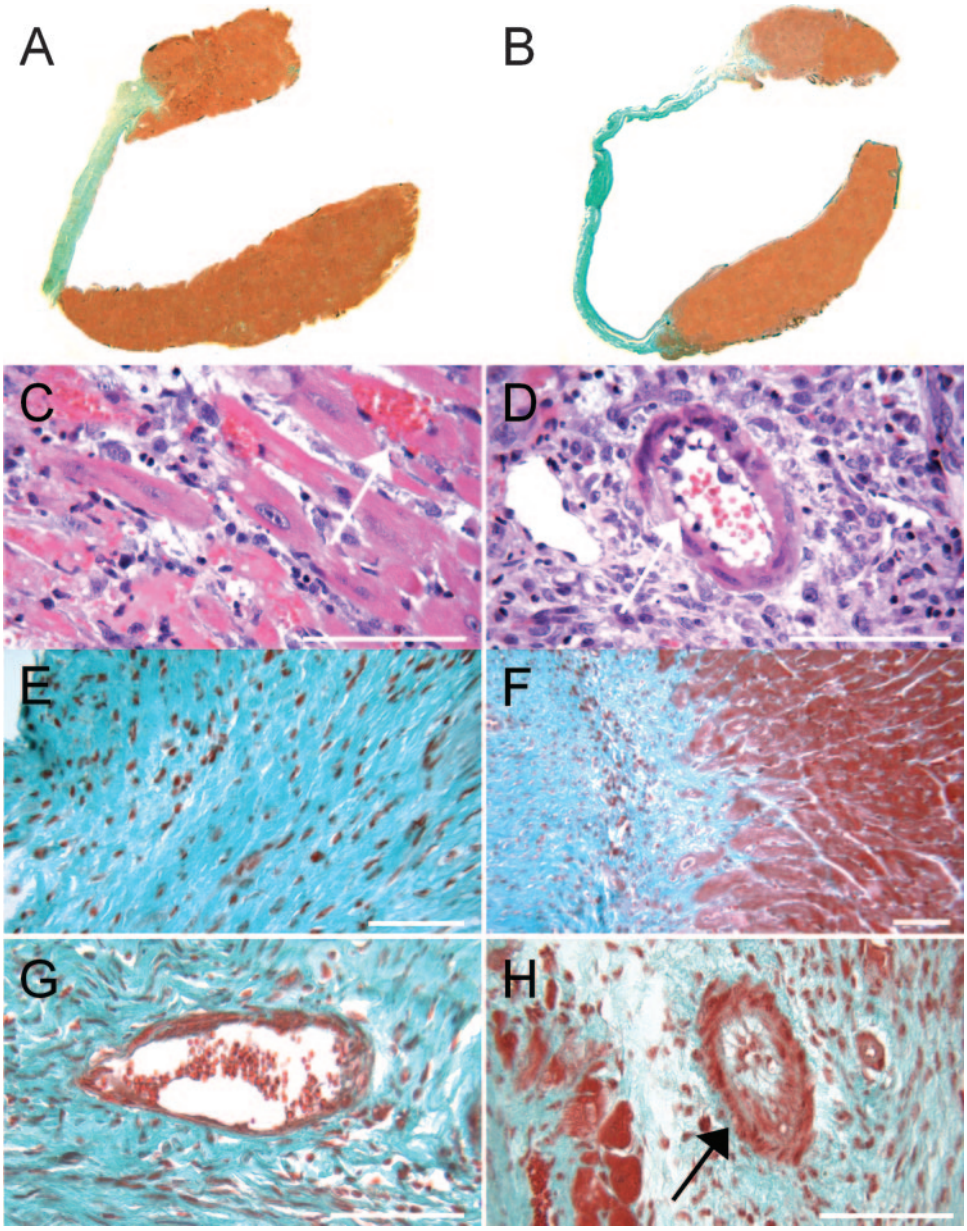

Fig. 4. *A*: 3-mm cryoinfarction at 8 wk [Masson's trichrome (MT) stain]. The infarct area is green. The infarct is smaller and thicker when compared with the 8-wk-old ligation infarct shown in *B*. *C* and *D*: HE staining of a 4-day-old cryoinfarct. Areas of hemorrhage (arrow) and a dense inflammatory infiltrate were observed (*C*). Furthermore, vascular lacunae were visible with endothelial discontinuities (arrow; *D*). Four weeks after cryoinfarction, a transmural, paucicellular scar had formed, with short transition zones to healthy myocardium (*E* and *F*, MT stain). At 8 wk, the LAD was patent in all cryoinfarcted animals (*G*, MT stain); in contrast, obliteration of the LAD and larger vessels was invariably observed in the ligation infarcts (arrow; *H*, MT stain). Bars = 100 μm.

was accompanied by an increase in the early relaxation parameter τ. However, as mentioned above, no significant increase was seen in LVEDP in the cryoinfarction groups in contrast with coronary ligation (Table 2). A trend toward further deterioration of LV dP/dt_{min} and τ was observed in the 3-mm cryoinfarction group between 4 and 8 wk, so that at 8 wk LV dP/dt_{min} and τ were similar in the 3-mm cryoinfarction and ligation groups.

Echocardiography. Two-dimensional guided M-mode images were obtained at baseline and 4 or 8 wk after infarction (Fig. 7). Interobserver variability was −3.3 ± 0.8% and −3.2 ± 2.6% for LV lumen EDD and FS, respectively, indicating high reproducibility of the echo analysis.

Baseline lumen EDD was 3.7 ± 0.04 mm for all groups (data not shown in Table 3). Cryoinfarction did not result in LV dilation at 4 wk (Table 3 and Fig. 8). However, in the period between 4 and 8 wk, LV lumen EDD increased significantly in the 3-mm cryoinfarction group compared with the sham group. In contrast, coronary ligation caused marked LV dilation already at 4 wk, with only modest further LV dilation occurring between 4 and 8 wk (Fig. 8).

Baseline FS was 33.9 ± 0.6% for all groups (data not shown in Table 3). Global LV pump function as indicated by FS was significantly reduced compared with the sham group in both the cryoinfarction groups as well as in the ligation group after 4 wk. A further significant decline was observed after 8 wk in the 3-mm cryoinfarction group (Table 3).

Cardiomyocyte hypertrophy and relative LV mass. Cardiomyocyte transverse cross-sectional area was significantly increased in the 3-mm cryoinfarction group after 8 wk. However, this modest hypertrophy was not reflected in increased LV weight-to-tibia length ratio, likely due to the loss of viable tissue (Fig. 9). In the ligation groups, marked LV hypertrophy was observed already after 4 wk, which was reflected by a

Table 1. *Morphometric measurements*

	Cryoinfarction		
	2 mm	3 mm	Ligation
n			
4 wk	6	9	10
8 wk		10	11
Epicardial infarct length, mm			
4 wk	2.3±0.1	3.4±0.2*	4.5±0.4*†
8 wk		3.4±0.2	4.6±0.3†
Endocardial infarct length, mm			
4 wk	1.1±0.1	1.7±0.2	3.6±0.3*†
8 wk		1.8±0.2	3.8±0.3†
Infarct thickness, mm			
4 wk	0.36±0.03	0.35±0.03	0.20±0.03*†
8 wk		0.26±0.04§	0.11±0.01†‡
Infarct area, mm^2			
4 wk	0.80±0.08	1.31±0.17	1.76±0.20*
8 wk		1.16±0.11	1.54±0.14

Values are means ± SE; *n*, no. of animals. *$P < 0.05$ vs. corresponding 2-mm cryoinfarction; †$P < 0.05$ vs. corresponding 3-mm cryoinfarction; ‡$P < 0.05$ vs. corresponding 4 wk; §$P = 0.05$ vs. corresponding 4 wk.

Table 2. *Hemodynamic measurements*

	Cryoinfarction			
	Sham	2 mm	3 mm	Ligation
n				
4 wk	12	12	8	10
8 wk	8		11	20
HR, beats/min				
4 wk	531±18	522±6	502±12	555±9
8 wk	554±11		531±9	524±8
LVEDP, mmHg				
4 wk	4±1	3±2	5±1	11±2*†‡
8 wk	5±1		5±1	8±1‡
LVSP, mmHg				
4 wk	101±3	84±4*	85±5*	88±3*
8 wk	83±5§		85±2	84±2
DAP, mmHg				
4 wk	71±3	62±4	66±5	68±3
8 wk	59±4§		67±3	58±2§

Values are means ± SE; *n*, no. of animals. HR, heart rate; LVEDP, left ventricular (LV) end-diastolic pressure; LVSP, LV systolic pressure; DAP, diastolic aortic pressure. *$P < 0.05$ vs. corresponding sham; †$P < 0.05$ vs. corresponding 2-mm cryoinfarction; ‡$P < 0.05$ vs. corresponding 3-mm cryoinfarction; §$P < 0.05$ vs. corresponding 4 wk.

marked increase in cardiomyocyte transverse cross-sectional area and LV weight-to-tibia length ratio (Fig. 9).

Pulmonary congestion and right ventricular hypertrophy. Signs of LV backward failure such as pulmonary congestion and right ventricular hypertrophy were absent in the cryoinfarction groups after 4 or 8 wk (Fig. 9). In contrast, wet lung weight-to-tibia length ratios and right ventricular weight-to-tibia length ratios were increased in the ligation group at 8 wk compared with the sham and 3-mm cryoinfarction groups.

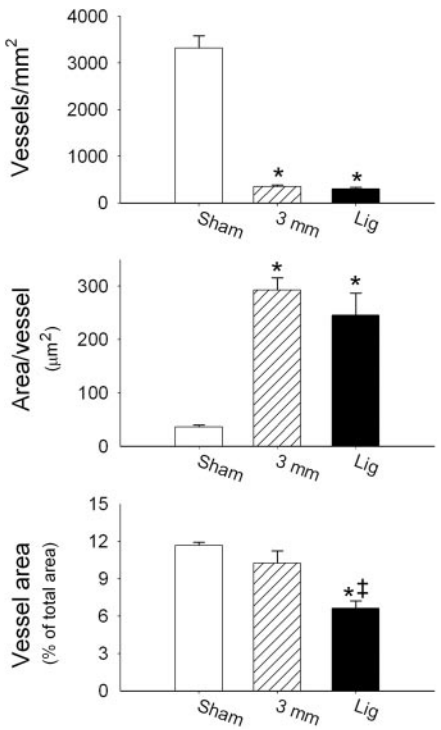

Fig. 5. Vessel density and vessel area at 8 wk. Numbers of vessels per millimeter squared declined significantly in both infarction groups compared with the sham group. Average area per vessel increased significantly in both infarct groups. This resulted in a significant smaller total vessel area per total tissue area in the ligation group compared with the sham and 3-mm cryoinfarction groups. *$P < 0.05$ vs. corresponding sham; ‡$P < 0.05$ vs. corresponding 3 mm.

DISCUSSION

In the present study, we describe the functional and structural effects of cryoinjury-induced MI in the mouse and compared these with the effects of LAD ligation. Although cryoinjury has been previously described in mice (1, 14, 15), this is the first study to directly compare both models using echocardiography and LV catheterization and to evaluate different sizes of cryoinjury. The principal findings of this study were *1*) cryoinfarction in the mouse is a feasible and highly standardized method to create MI with low peri- and postoperative mortality; *2*) cryoinfarction results in macrovascular reperfusion with microvascular reperfusion occurring selectively along the endocardial borders; and *3*) cryoinfarction results in loss of contractility and in diastolic dysfunction to a similar degree as LAD ligation after 8 wk with, however, more modest LV remodeling and no signs of overt backward LV failure.

Previous studies. The induction of MI by coronary ligation in mice was initially described 20 years ago (26). However, the chronic effects of LAD ligation on LV function and remodeling have only more recently been documented in detail. In a previous study (12), ketamine-pentobarbital anesthesia was used, resulting in lower HRs (230–270 beats/min) than reported in the present study under isoflurane anesthesia (500–550 beats/min), which is in the range of HRs (450–650 beats/min) that we (4) and others (10, 25) observed in mice under awake conditions. Therefore, the present study is, to our knowledge, the first study that presents echocardiographic and hemodynamic data of a chronic MI mouse model under physiological conditions obtained by the use of isoflurane anesthesia.

In recent years, cryoinjury has been described in animals such as the rat (2, 9) and rabbit (21). Cryoinfarction in the mouse has only been described in three reports from the same research group (1, 14, 15). In these studies, a cryoprobe was

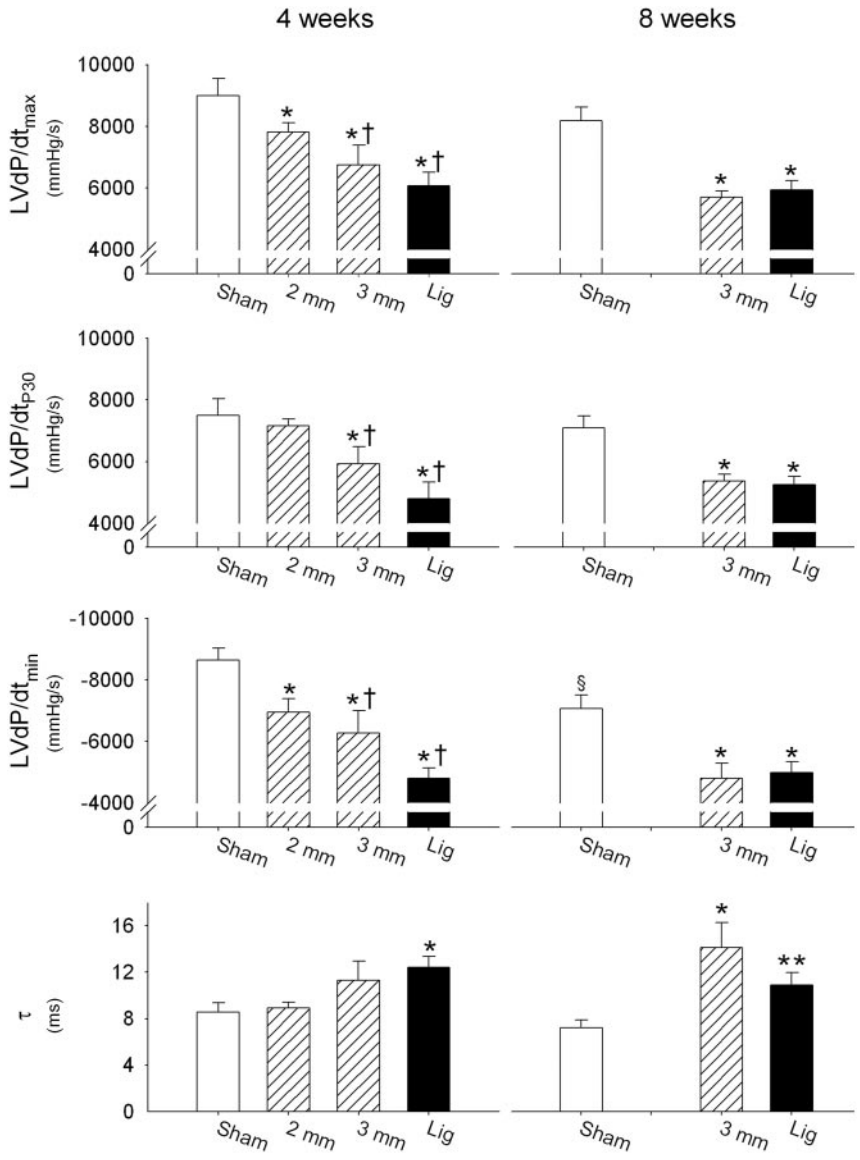

Fig. 6. Systolic function parameters. LV dP/dt_{max}, maximum rate of rise of left ventricular (LV) pressure; LV dP/dt_{P30}, first derivative of LV pressure at a pressure of 30 mmHg; LV dP/dt_{min}, maximum rate of fall of LV pressure; τ, time constant of LV pressure decay. *$P < 0.05$ vs. corresponding sham; †$P < 0.05$ vs. corresponding 2 mm; ‡$P < 0.05$ vs. corresponding 3 mm; §$P < 0.05$ vs. corresponding 4 wk; **$P = 0.06$ vs. corresponding sham.

used that was precooled in liquid nitrogen. The disadvantage of using a precooled probe is that several applications are necessary to obtain the desired effect because of rapid defrosting. The uniformity of the injury may, therefore, be less than when using the probe described in the present study. We used a commercially available probe with the capability of continuous freezing resulting in a well-defined area of necrosis.

In the three studies mentioned above (1, 14, 15), either echocardiography or LV catheterization was used as a functional end point, but both methods were never applied simultaneously. Our study is, therefore, the first to describe the effects of cryoinjury in a mouse model using both echocardiography and LV catheterization and to compare the outcomes directly with the more established model of LAD ligation.

Pathophysiology of the cryoinfarction model. The pathophysiology of cryoinjury differs from LAD ligation because it results in acute cell death at the moment of freezing without concomitant ischemia. The injury caused by the freezing process probably results from the mechanical forces induced by formation of ice crystals both in the intracellular and extracellular space and inside the vasculature (7).

The length of the epicardial cryoinfarct borders correlated closely with the size of the probe used, demonstrating the high predictability of the method (Table 1). Endocardial infarct length was about half of the epicardial length corresponding with the cone-shaped lesion observed macroscopically.

Histology of the cryoinfarct area at 2 and 4 days postinfarction showed large areas of hemorrhage in the infarct center, consistent with findings by others (2, 5). Thioflavin S staining showed large no-reflow zones within the infarct center corresponding with microvascular damage. However, the macrovasculature was patent. This was confirmed by Unisperse blue staining: capillary reperfusion was selectively observed along endocardial borders. In contrast, the LAD and larger vessels were all reperfused. This likely led to the larger relative vessel area compared with ligation infarcts at 8 wk (Fig. 5). These findings might explain why infarct remodeling was less outspoken in the cryoinfarction model, because it has been pro-

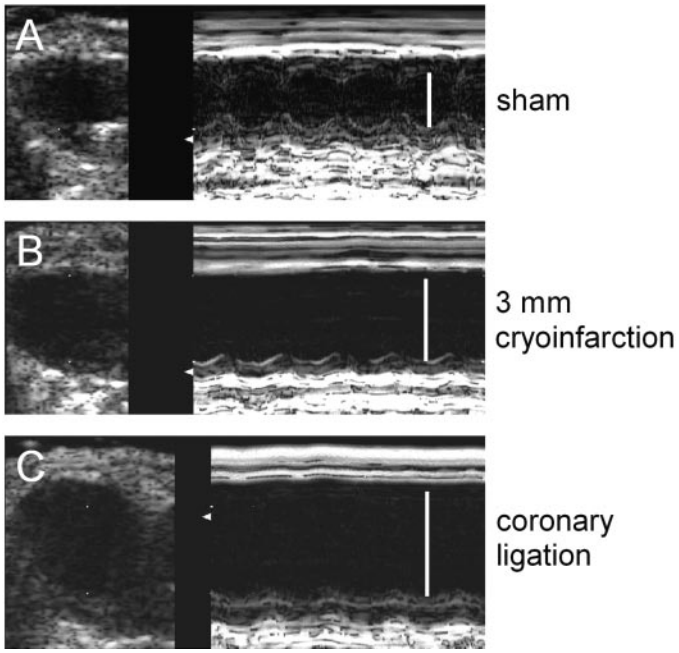

Fig. 7. Representative two-dimensional (*left*) and corresponding M-mode images (*right*) of a long-axis view 8 wk after sham operation (*A*), 3-mm cryoinfarction (*B*), or coronary ligation (*C*). Cryoinfarction resulted in akinesis of the anterior wall and modest LV dilation. Coronary ligation resulted in anterior akinesis and marked LV dilation. The vertical line indicates the end-diastolic lumen diameter.

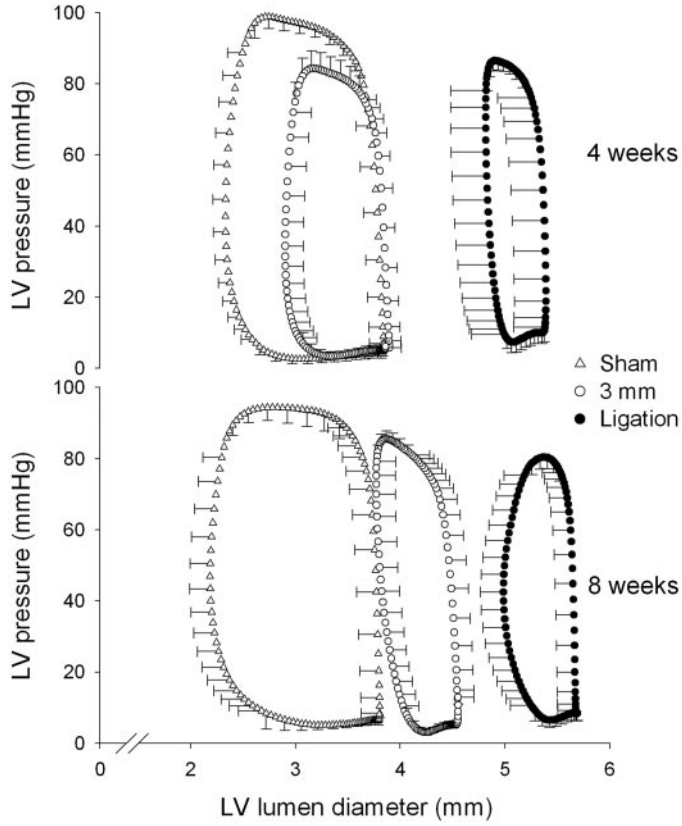

Fig. 8. Pressure-diameter relations were constructed by combining echocardiography and LV pressure data. Electrocardiographic gating was used to synchronize both signals. It can be appreciated that from 4 to 8 wk, a rightward shift occurred in the 3-mm cryoinfarction group, indicating ongoing adverse remodeling.

posed that the blood-filled vasculature can act as a "scaffolding" that supports surrounding necrotic myocardium (13).

LV function and remodeling after cryoinfarction. Four weeks after cryoinjury, FS was substantially reduced in the 2- and 3-mm cryoinfarction groups. This was accompanied by a significant effect on contractility, as assessed by LV dP/dt_{max} and the afterload-independent variable LV dP/dt_{P30} in the 3-mm cryoinfarction group, and by a significant effect on diastolic function, as reflected by LV dP/dt_{min} and τ. Because the decrease in LV dP/dt_{P30} was only modest in the 2-mm cryoinfarction group, we chose to follow only the 3-mm cryoinfarction group up to 8 wk.

At 8 wk, the effects on these parameters were similar in the 3-mm cryoinfarction and ligation groups. It is therefore somewhat surprising that despite the extent of these changes, only modest LV remodeling and no signs of backward failure were observed after cryoinfarction contrasting with the marked alterations in the ligation model.

After 8 wk, a significant increase in cardiomyocyte cross-sectional area in the 3-mm cryoinfarction group was observed, although LV weight-to-tibia length ratios were not increased. However, it should be taken into account that because of tissue loss in the infarct area, initially a decrease in LV weights occurs, which likely explains this paradoxical observation.

In the sham group, a small but significant effect was seen in LV dP/dt_{min} at 8 wk compared with 4 wk, suggesting slight diastolic dysfunction, although this may have been caused in

Table 3. *Echocardiography*

		Cryoinfarction		
	Sham	2 mm	3 mm	Ligation
n				
4 wk	12	12	9	9
8 wk	6		10	19
End-diastolic lumen diameter, mm				
4 wk	3.9±0.1	4.0±0.1	4.0±0.1	5.4±0.3*†‡
8 wk	3.9±0.2		4.6±0.2*	5.7±0.2*‡
Fractional shortening, %				
4 wk	34.0±0.8	22.3±1.4*	20.8±1.7*	10.3±1.6*†‡
8 wk	34.9±4.1		14.4±2.2*§	9.6±1.0*‡

Values are means ± SE; *n,* no. of animals. *$P < 0.05$ vs. corresponding sham; †$P < 0.05$ vs. corresponding 2-mm cryoinfarction; ‡$P < 0.05$ vs. corresponding 3-mm cryoinfarction; §$P < 0.05$ vs. corresponding 4 wk.

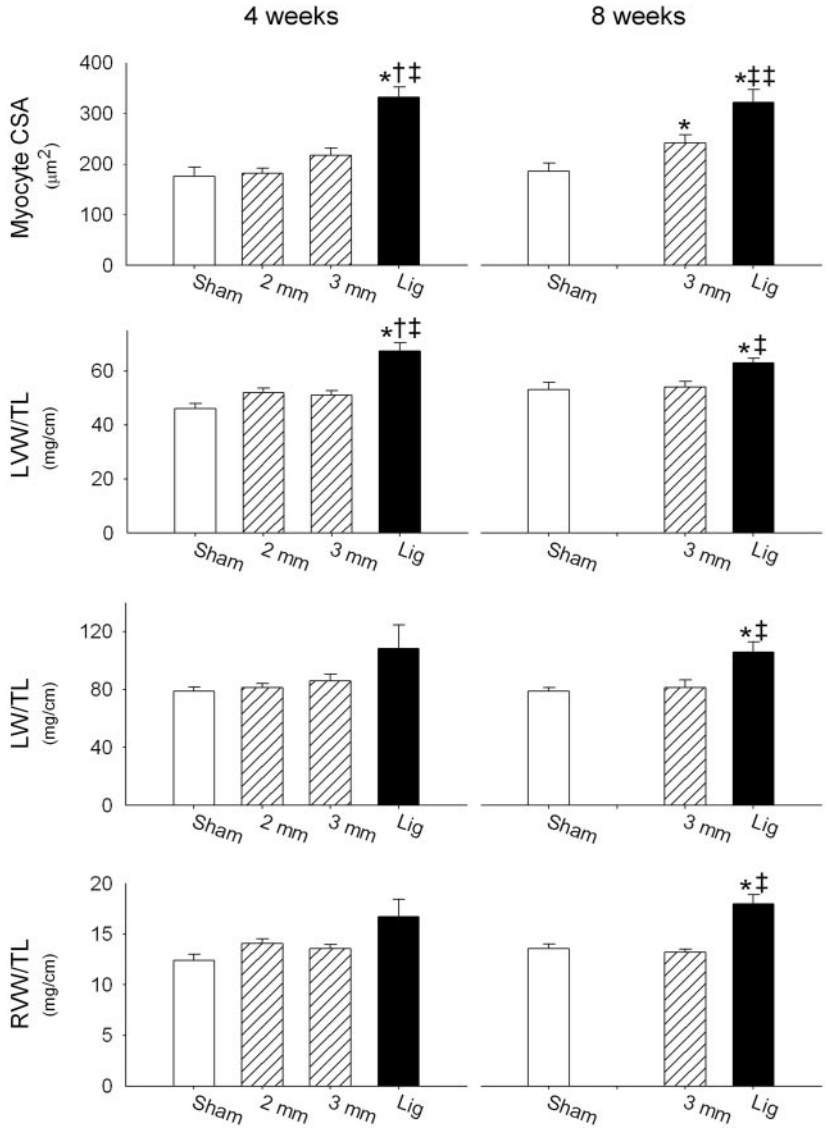

Fig. 9. Parameters of LV remodeling and LV backward failure. For the 3-mm cryoinfarction group, a significant increase in myocyte transverse cross-sectional area (CSA) is observed at 8 wk. However, LV weight-to-tibia length ratio (LVW/TL) is not increased in contrast with coronary ligation, where significant cardiomyocyte and LV hypertrophy is observed already at 4 wk. No signs of LV backward failure were observed after cryoinfarction. In contrast, significant increases in wet lung weight-to-tibia length ratio (LW/TL) and right ventricular weight-to-tibia length ratio (RVW/TL) were observed 8 wk after coronary ligation, indicating pulmonary congestion and right ventricular hypertrophy. $*P < 0.05$ vs. corresponding sham; †$P < 0.05$ vs. corresponding 2 mm; ‡$P < 0.05$ vs. corresponding 3 mm; ‡‡$P = 0.10$ vs. corresponding 3 mm. No significant differences were found between the 4- and 8-wk time points.

part by the lower LVSP in the 8-wk sham group as the less load-dependent parameter τ was not significantly changed. To our knowledge, no studies have investigated the effect of thoracotomy in the mouse on hemodynamic function at two time points. An effect of relief of pericardial constraint after pericardectomy could play a role, as it has been described that LV dilation and hypertrophy occurs in humans after pericardectomy (22). However, in the present study, no LV remodeling was observed in the sham group at 8 wk and no significant differences were observed between sham and control animals at 8 wk. Another possible explanation would be that adhesions in the area of surgery exerted a negative effect.

In a previous cryoinfarction study (1) using a 4-mm cryoprobe, more adverse remodeling was reported after 4 wk compared with the 3-mm probe in our study. This corresponded with larger infarct areas reported (1). However, in our study, more systolic and diastolic LV dysfunction was observed after 4 wk using the 3-mm probe. This apparent discrepancy could be due in part to differences in anesthesia. In the present study, isoflurane was used, whereas the agent tribromoethanol was used in the other study.

In our model, the largest probe used was 3 mm in diameter because larger probe sizes did not fit well with our thoracotomy, because the area of freezing extends far beyond the actual probe size. This effect is not seen when a precooled probe was used, as in the study mentioned above (1). Because, in our study, a significant adverse effect on LV function was found using a 3-mm probe already at 4 wk, we did not explore the effects of larger freeze injuries.

Methodological considerations. No overt heart failure was seen after cryoinjury, likely due to the smaller infarct size compared with coronary ligation. We therefore feel that the cryoinfarction model should not be used to replace existing heart failure models. Rather, it could serve as a model for the assessment of therapeutic interventions aimed at reducing cardiac remodeling and improving cardiac function after infarction, such as therapies aimed at cardiac regeneration using progenitor cells or growth factors.

The follow-up period in this study was 8 wk. Probably the 8-wk period is adequate to assess the degree of LV remodeling or the effect of therapeutic interventions after cryoinfarction. Earlier studies reported marked effects on LV remodeling after

4 wk in a cryoinfarction model (1) or 6 wk in a LAD ligation model (12). Our coronary ligation model resulted in a significant degree of LV remodeling after 4 wk. However, because adverse remodeling in the cryoinfarction group only became apparent in the period between 4 and 8 wk, longer follow-up periods may be studied in the future to assess the long-term effects of cryoinfarction.

Future studies. The cryoinfarction model described is potentially an ideal model to evaluate interventions aimed at restoration of cardiac function or cardiac regeneration after MI without a setting of overt heart failure. Thus this model would be useful in cell transplantation studies (9, 15, 17, 21) because *1*) cells could then be easily injected at well-defined locations, *2*) macrovascular reperfusion could be beneficial for cellular repair, *3*) the repair process could be studied in an organized and very reproducible way, and *4*) the mouse model would offer the possibility to investigate multiple (transgenic) cell types.

In conclusion, this study describes the functional and histological characteristics of a chronic, murine model of cardiac cryoinfarction and compares these with the classical model of MI through permanent coronary ligation. The results show that cryoinfarction is a technique with high periprocedural survival resulting in reproducible infarcts leading to significant LV dysfunction and a modest degree of ventricular remodeling over a period of 8 wk. These features make our cryoinfarction model a useful tool for analysis of functional effects of various interventions for cardiac regeneration such as cell therapy.

GRANTS

This study was supported by The Netherlands Heart Foundation Established Investigator Stipend 2000T038 (to D. J. Duncker), by ZON-MW Agiko Stipends 920-03-191 (to E. J. van den Bos) and 920-03-291 (to B. M. E. Mees), and by an International Society for Heart and Lung Transplantation 2003 Research Fellowship Award (to E. J. van den Bos).

REFERENCES

1. **Brede M, Roell W, Ritter O, Wiesmann F, Jahns R, Haase A, Fleischmann BK, and Hein L.** Cardiac hypertrophy is associated with decreased eNOS expression in angiotensin AT_2 receptor-deficient mice. *Hypertension* 42: 1177–1182, 2003.
2. **Ciulla MM, Paliotti R, Ferrero S, Braidotti P, Esposito A, Gianelli U, Busca G, Cioffi U, Bulfamante G, and Magrini F.** Left ventricular remodeling after experimental myocardial cryoinjury in rats. *J Surg Res* 116: 91–97, 2004.
3. **De Waard MC, van Deel ED, Merkus D, van Haperen R, de Crom R, and Duncker DJ.** Beneficial effect of exercise training on cardiac function is lost in mice that overexpress endothelial NO synthase (Abstract). *Circulation* 110: III–299, 2004.
4. **Duncker DJ, van Haperen R, van Deel ED, de Waard MC, Mees B, and de Crom R.** Endothelial nitric oxide synthase in cardiovascular homeostasis and disease. In: *The Physiological Genomics of the Critically Ill Mouse*, edited by Ince C. Dordrecht, The Netherlands: Kluwer, 2004, p. 291–310.
5. **Huwer H, Nikoloudakis N, Rissland J, Vollmar B, Menger MD, and Schafers HJ.** In vivo analysis of microvascular injury after myocardial cryothermia. *J Surg Res* 79: 1–7, 1998.
6. **Kamphoven JH, Stubenitsky R, Reuser AJ, Van Der Ploeg AT, Verdouw PD, and Duncker DJ.** Cardiac remodeling and contractile function in acid α-glucosidase knockout mice. *Physiol Genomics* 5: 171–179, 2001.
7. **Mazur P.** Cryobiology: the freezing of biological systems. *Science* 168: 939–949, 1970.
8. **Michael LH, Entman ML, Hartley CJ, Youker KA, Zhu J, Hall SR, Hawkins HK, Berens K, and Ballantyne CM.** Myocardial ischemia and reperfusion: a murine model. *Am J Physiol Heart Circ Physiol* 269: H2147–H2154, 1995.
9. **Murry CE, Wiseman RW, Schwartz SM, and Hauschka SD.** Skeletal myoblast transplantation for repair of myocardial necrosis. *J Clin Invest* 98: 2512–2523, 1996.
10. **Palakodeti V, Oh S, Oh BH, Mao L, Hongo M, Peterson KL, and Ross J Jr.** Force-frequency effect is a powerful determinant of myocardial contractility in the mouse. *Am J Physiol Heart Circ Physiol* 273: H1283–H1290, 1997.
11. **Passier R, Zeng H, Frey N, Naya FJ, Nicol RL, McKinsey TA, Overbeek P, Richardson JA, Grant SR, and Olson EN.** CaM kinase signaling induces cardiac hypertrophy and activates the MEF2 transcription factor in vivo. *J Clin Invest* 105: 1395–1406, 2000.
12. **Patten RD, Aronovitz MJ, Deras-Mejia L, Pandian NG, Hanak GG, Smith JJ, Mendelsohn ME, and Konstam MA.** Ventricular remodeling in a mouse model of myocardial infarction. *Am J Physiol Heart Circ Physiol* 274: H1812–H1820, 1998.
13. **Reffelmann T, Hale SL, Dow JS, and Kloner RA.** No-reflow phenomenon persists long-term after ischemia/reperfusion in the rat and predicts infarct expansion. *Circulation* 108: 2911–2917, 2003.
14. **Roell W, Fan Y, Xia Y, Stoecker E, Sasse P, Kolossov E, Bloch W, Metzner H, Schmitz C, Addicks K, Hescheler J, Welz A, and Fleischmann BK.** Cellular cardiomyoplasty in a transgenic mouse model. *Transplantation* 73: 462–465, 2002.
15. **Roell W, Lu ZJ, Bloch W, Siedner S, Tiemann K, Xia Y, Stoecker E, Fleischmann M, Bohlen H, Stehle R, Kolossov E, Brem G, Addicks K, Pfitzer G, Welz A, Hescheler J, and Fleischmann BK.** Cellular cardiomyoplasty improves survival after myocardial injury. *Circulation* 105: 2435–2441, 2002.
16. **Salto-Tellez M, Yung Lim S, El-Oakley RM, Tang TP, Almsherqi ZA, and Lim SK.** Myocardial infarction in the C57BL/6J mouse: a quantifiable and highly reproducible experimental model. *Cardiovasc Pathol* 13: 91–97, 2004.
17. **Suzuki K, Murtuza B, Beauchamp JR, Smolenski RT, Varela-Carver A, Fukushima S, Coppen SR, Partridge TA, and Yacoub MH.** Dynamics and mediators of acute graft attrition after myoblast transplantation to the heart. *FASEB J* 18: 1153–1155, 2004.
18. **Svenson KL, Bogue MA, and Peters LL.** Invited review: Identifying new mouse models of cardiovascular disease: a review of high-throughput screens of mutagenized and inbred strains. *J Appl Physiol* 94: 1650–1659, 2003.
19. **Tanaka N, Dalton N, Mao L, Rockman HA, Peterson KL, Gottshall KR, Hunter JJ, Chien KR, and Ross J Jr.** Transthoracic echocardiography in models of cardiac disease in the mouse. *Circulation* 94: 1109–1117, 1996.
20. **Taylor CB, Davis CB Jr, Vawter GF, and Hass GM.** Controlled myocardial injury produced by a hypothermal method. *Circulation* 3: 239–253, 1951.
21. **Taylor DA, Atkins BZ, Hungspreugs P, Jones TR, Reedy MC, Hutcheson KA, Glower DD, and Kraus WE.** Regenerating functional myocardium: improved performance after skeletal myoblast transplantation. *Nat Med* 4: 929–933, 1998.
22. **Tischler MD, Rowan M, and LeWinter MM.** Increased left ventricular mass after thoracotomy and pericardiotomy. A role for relief of pericardial constraint? *Circulation* 87: 1921–1927, 1993.
23. **Van der Velden J, Merkus D, Klarenbeek BR, James AT, Boontje NM, Dekkers DH, Stienen GJ, Lamers JM, and Duncker DJ.** Alterations in myofilament function contribute to left ventricular dysfunction in pigs early after myocardial infarction. *Circ Res* 95: e85–e95, 2004.
24. **Virag JI and Murry CE.** Myofibroblast and endothelial cell proliferation during murine myocardial infarct repair. *Am J Pathol* 163: 2433–2440, 2003.
25. **Yang XP, Liu YH, Rhaleb NE, Kurihara N, Kim HE, and Carretero OA.** Echocardiographic assessment of cardiac function in conscious and anesthetized mice. *Am J Physiol Heart Circ Physiol* 277: H1967–H1974, 1999.
26. **Zolotareva AG and Kogan ME.** Production of experimental occlusive myocardial infarction in mice. *Cor Vasa* 20: 308–314, 1978.